LTE Network Radio Planning

Igor R. Maravić and Aleksandar M. Nešković

***Abstract*—In this paper different ways of planning the radio resources within an LTE network are analyzed. All simulations were carried out using 3GPP recommendations. Soft frequency reuse (SFR), soft fractional frequency reuse (SFFR) and hard fractional frequency reuse (HFFR) radio resource allocation schemes are compared to fixed frequency reuse 1 (R1) and reuse 3 (R3) radio resource allocation schemes. An optimum way of planning radio resources in a LTE network is proposed at the end of paper.**

***Keywords*—LTE, radio planning, simulation.**

I. Introduction

To meet customer demands for high data rates, LTE systems anticipate the highest possible frequency re-use. This means that the goal of LTE networks is to use frequency reuse of one, or as close to one as possible. Spatial frequency reuse of one implies that all base stations (BSs) in the network transmit on all physical resource blocks (PRBs) simultaneously [1]. The advantage of this radio resource management (RRM) scheme is a significant increase in system capacity. However, the big downside of this RRM scheme is a significant degradation of performances that edge users experience. Performance degradation is induced by large interference, which originates from other cells in the network [2]. Advanced RRM algorithms are necessary in order to preserve the full potential of the orthogonal frequency division multiplex (OFDM) in a dense reuse environment [3].

With the aim of attaining high spectral efficiency, but also reducing intercellular interference for edge users, this paper is considering a flexible use of reuse factors. Different RRM algorithms were examined and compared. Our goal was to find the algorithm with the best compromise between obtained flow rate, and intercellular interference at the cell edge.

Section II describes existing LTE RRM techniques. Section III presents used simulator and the used simulation parameters. Section IV presents the obtained results.

II. Radio Resource Allocation Schemes

To be able to compare the different RRM schemes, a radio resource utilization (RRU) factor is introduced. It is defined as follows [4]:

$$U = \frac{\sum_{i \in N_{PRB}} P_i}{N_{PRB} P_{max}}, \qquad (1)$$

where P_{max} represents the maximum available power per PRB, P_i represents the maximum power that can be used by the i-th PRB and N_{PRB} represents the number of PRBs that are available in an assigned frequency band.

A. Fixed Frequency Reuse

Fixed frequency reuse schemes with reuse factor of 1 (R1) and with reuse factor of 3 (R3) imply fixed power per each available PRB. Used power per PRB equals the maximum available power per PRB (P_{max}).

The main problem of R1 RRM is the strong intercellular interference as a consequence of the fact that all BSs are transmitting the signal over the whole frequency range with maximal available power. This is the highest possible RRU that one RRM could obtain, according to (1).

The aforementioned R1 is suitable for scenarios with low traffic loads while under heavy traffic loads the interference becomes too high, especially on the cell edge.

R3 RRM uses a third of the available bandwidths in each cell. Based on (1), RRU factor for this RRM is 1/3. Using this RRM, interference is reduced, thus improving the throughput for the users on the cell border, but the overall data throughput in the cell is much lower.

B. Soft Frequency Reuse (SFR)

The soft frequency reuse (SFR) scheme, shown in Fig. 1, divides the whole available spectrum in each cell into two groups – major and minor subcarrier groups [3]. The major subcarrier group usually uses one-third of the available spectrum, and it is planned as R3.

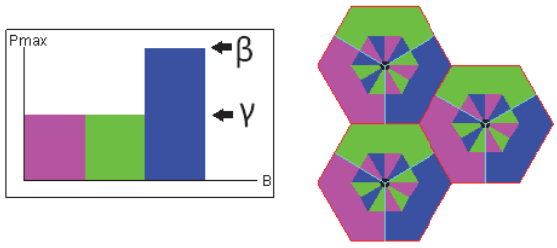

Fig 1. Power distribution within the spectrum and the cell appearance in case of SFR.

In this subcarrier group eNodeB (eNB) transmits the signal with full power. The minor subcarrier group covers the remaining two-thirds of the available spectrum. In this subcarrier group eNB transmits a signal with power of $\gamma \cdot P_{max}$, where $\gamma \leq 1$.

When implementing SFR users are divided depending on their location in the cell. They are split into two groups – central users and border users. This is very important because central users can obtain resources from the minor subcarrier group only, while the border users obtain resources from the major subcarrier group.

I. Maravić, Innovation center, School of Electrical Engineering, University of Belgrade, Bulevar kralja Aleksandra 73, 11120 Belgrade, Serbia (telephone: 381-66-413123, e-mail: igorm@etf.rs)

A. Nešković, School of Electrical Engineering, University of Belgrade, Bulevar kralja Aleksandra 73, 11120 Belgrade, Serbia (telephone 381-64-1115983; fax: 381-11-3218399; e-mail: neshko@etf.rs)

C. *Fractional Frequency Reuse (FFR)*

Fractional frequency reuse (FFR) scheme divides the available spectrum in each cell into two zones – inner and outer [3]. The inner zone uses a bandwidth of $\delta \cdot B$, where B represents the total available bandwidth and $\delta \leq 1$. In this spectrum zone eNB transmits a signal with a power of $\alpha \cdot P_{max}$, where $\alpha \leq 1$. The spectrum in the inner zone is planned as R1. The outer zone uses the remaining bandwidth. Depending on how the outer zone is planned, two FFR types can be distinguished - *Soft* FFR (SFFR) and *Hard* FFR (HFFR).

In HFFR, shown in Fig. 2, the outer zone is planed as R3. In this zone eNB transmits a signal with a power of P_{max}. Users are divided into two groups, depending on their location in the cell. PRBs from the inner zone are allocated to users in the cell centre. PRBs from the outer spectrum zone are allocated to the users that reside on the cell border.

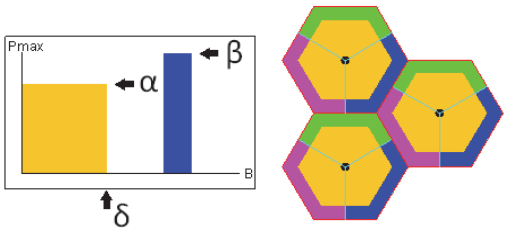

Fig. 2. Power distribution within the spectrum and the cell appearance in case of HFFR.

In SFFR, shown in Fig. 3, the outer zone is planned as SFR. As in HFFR, in SFFR users are divided into two groups. Users in the cell centre are obtaining resources from the inner zone and from the minor subcarrier group of the outer zone, while the users on the cell edge are using resources from the major subcarrier group of the outer spectrum zone.

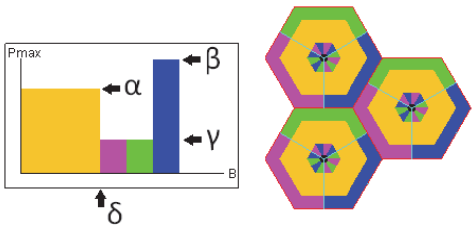

Fig. 3. Power distribution within the spectrum and the cell appearance in case of SFFR.

III. Simulator

For research purposes, a software LTE simulator was implemented by 3GPP standards. LTE simulator was completely developed in Java. Its source code can be freely downloaded from [5].

From the user interface (UI), shown in Fig. 4, all aforementioned parameters, i.e. α, β, γ, δ and intercell border (ICB), can be changed freely via sliders. Changing any of those values is immediately transferred to the picture of spectrum power distribution and to the picture of LTE network.

Simulated LTE network contains a central cell and eighteen cells that are arranged in a circle around the central cell. Users are deployed in a central cell only and thus only central cell statistics are observed.

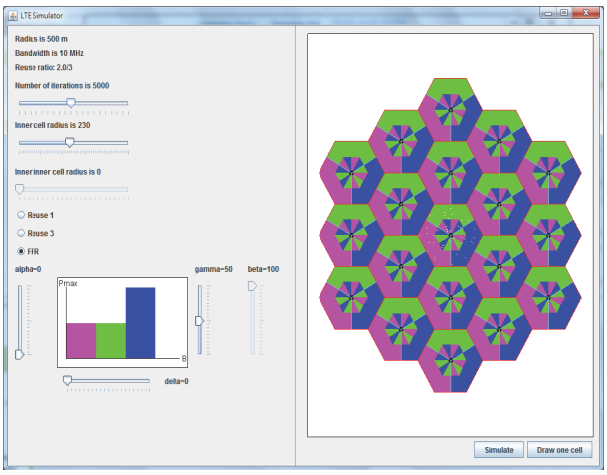

Fig. 4. Simulator's UI.

Simulations are conducted through series of independent snapshots. In each snapshot users are randomly deployed in a central cell. Depending on experienced propagation conditions, resources are allocated to users. At the end of each snapshot, statistics for all users are collected and at the end of the simulation the mean values of all collected data are calculated. To obtain more precise statistics, simulation should iterate through as many as possible snapshots.

All the simulations were carried out with the parameters presented in Table 1. Besides those parameters, it was assumed that the spectrum width is 10MHz. In this case, according to [6], the maximum number of PRBs is 50 (the spectrum width of a single PRB is 180kHz). A 4-bit channel quality indicator (CQI), defined in [7] was used. According to the user's CQI, simulator's scheduler decided which modulation it should use for the given user. Scheduler's goal was to use modulation that gives the highest throughput, for the propagation conditions that user experience. Dependency between signal-interference to noise ratio (SINR) and obtained throughput, as well as the relationship between SINR and block error rate (BLER), for a given modulation were taken from [8]. A fixed width of 10MHz was used (the same as in [1] and [2]), despite the fact that the bandwidth in LTE may have several different values. The results obtained for a system with a bandwidth of 10MHz could be applied to systems with other bandwidth widths. In those cases, the total achieved bandwidth should be properly scaled in accordance with the available number of PRBs.

IV. Simulation Results

LTE network simulations were conducted for R1, R3, SFR, SFFR and HFFR allocation schemes. Results that were obtained for R1 and R3 allocation schemes were referent and all other simulation results were compared with them. The simulation results are presented together with the total cell throughput and average PRB throughput as a function of distance from the cell centre. To provide more reliable results, all simulations iterated through 5000 independent snapshots.

Parameters γ and ICB were varied in SFR case, parameters α, γ, δ and ICB were varied in SFFR case and parameters α, δ and ICB were varied in HFFR case.

TABLE 1: MACRO CELL SIMULATION PARAMETERS [4].

Parameter	***Assumption***	
Cellular Layout	Hexagonal grid, 19 cell sites, 3 sectors per site	
Cell radius	500m	
Distance-dependent path loss	$L=128.1dB + 37.6 \log_{10}(R)$, where R represents user distance from TX, in kilometres	
Shadowing standard deviation	$\sigma = 8$ dB	
Shadowing correlation	Between cells	0.5
	Between sectors	1.0
Antenna pattern (horizontal)	$A(\theta) = -\min\left[12\left(\frac{\theta}{\theta_{3dB}}\right)^2, A_m\right]$ $\theta_{3dB} = 70°$, $A_m = 20$ dB	
Total signal attenuation	$L - A(\theta) - shadowing$ (*shadowing* has a Gaussian distribution with standard deviation σ)	
Carrier Frequency / Bandwidth	2GHz / 10MHz	
Total BS TX power (*Ptotal*)	46dBm - 10MHz carrier	
Inter-cell interference modeling	DL: BS TX, from other cells, radiate maximum power = *Ptotal*	
Uniform user distribution over cell area		
Minimal user distance from BS	>= 35 meters	

Values of α, γ, δ and ICB that were used in simulations, as well as total achieved throughputs per cell for those values, are given in Table 2.

The achieved results for different values of α, in HFFR and SFFR cases, are shown in Fig. 5 and Fig. 6, respectively. From those figures it can be noticed that this parameter does not affect the achieved throughput per PRB. Besides that it is observed that the PRB throughput in the cell centre gravitates to PRB throughput for R1. On the cell border PRB throughput strives to achieve the PRB throughput in R3 case. In HFFR case, throughput gains on the cell border are significant, while the gains on the cell border for SFFR are negligible. Despite that, the overall throughput is much lower in HFFR than in SFFR. This is due to the fact that SFFR has a greater number of available PRBs than HFFR.

The achieved results for different values of γ, in SFR and SFFR cases, are shown in Fig. 7 and Fig. 8, respectively. From those figures it can be observed that for smaller values of γ a greater throughput per PRB is achieved on the cell border, and a lesser throughput is achieved in the cell centre, compared with the simulation results for R1. This is so because the resources from the minor subcarrier group have lower power, compared to the resources from R1 scheme, and they have to cope with the interference that originates from the major subcarrier groups of adjacent cells. With the increase of γ PRB throughput begins to pursue the PRB throughput from R1 simulation.

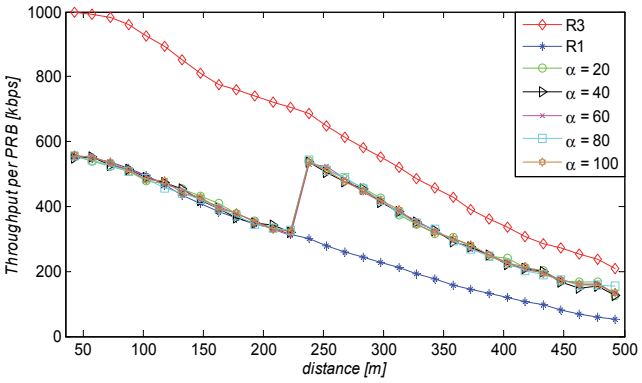

Fig. 5. The average throughput per PRB as a function of distance from BS, for HFFR with variation of α.

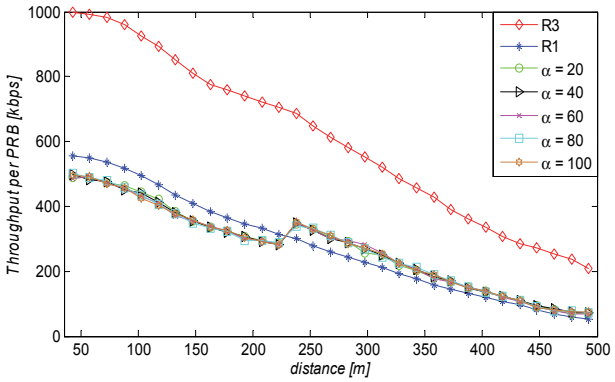

Fig. 6. The average throughput per PRB as a function of distance from BS, for SFFR with variation of α.

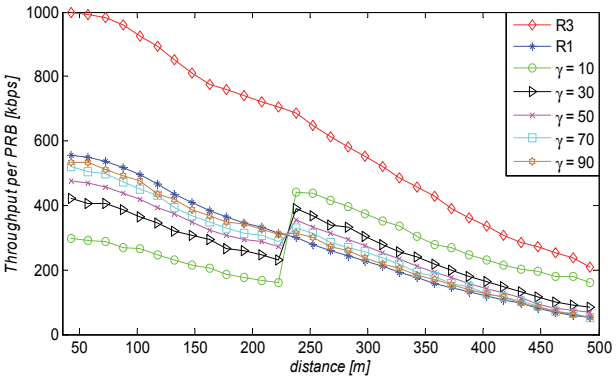

Fig. 7. The average throughput per PRB as a function of distance from BS, for SFR with variation of γ.

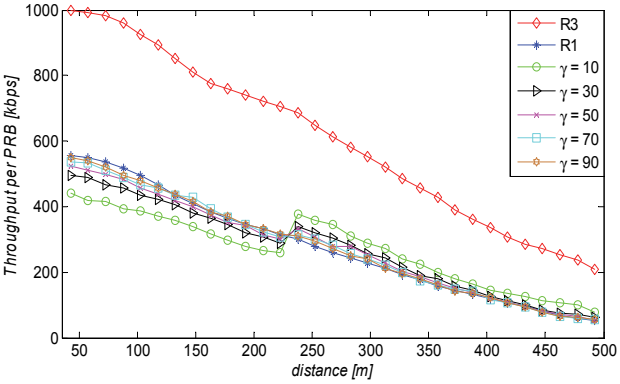

Fig. 8. The average throughput per PRB as a function of distance from BS, for SFFR with variation of γ.

TABLE 2: OVERALL THROUGHPUT ACHIEVED IN SIMULATIONS.

Allocation Scheme	*Overall throughput [Mbps]*				
R1	48.4				
R3	30.9				
SFFR with variation of α (β=1, γ=0.25, δ=0.5, ICB=230m, α={0.2, 0.4, 0.6, 0.8, 1})	47.0	47.0	46.9	47.1	46.8
HFFR with variation of α (β=1, γ=0, δ=0.5, ICB=230m,α={0.2, 0.4, 0.6, 0.8, 1})	41.1	41.0	41.2	40.8	41.2
SFR with variation of γ (α=0, β=1, δ=0, ICB=230m, γ={0.1, 0.3, 0.5, 0.7, 0.9})	39.5	41.9	43.3	44.1	44.8
SFFR with variation of γ (α=0.6, β=1, δ=0.5, ICB=230m, γ={0.1, 0.3, 0.5, 0.7, 0.9})	45.5	47.1	48.3	48.9	49.1
SFFR with variation of δ (α=0.6, β=1, γ=0.3, ICB=230m, δ={0.2, 0.3, 0.4, 0.6, 0.8})	44.9	45.6	45.8	47.1	47.5
HFFR with variation of δ (α=0.7, β=1, γ=0, ICB=230m, δ={0.1, 0.3, 0.5, 0.7, 0.9})	32.9	38.3	41.1	45.4	47.9
SFR with variation of ICB (α=0, β=1, γ=0.3, δ=0, ICB={0m,50m,100m,200m,300m})	46.6	46.6	45.7	44.0	40.8
SFFR with variation of ICB (α=0.6, β=1, γ=0.3, δ=0.5, ICB={50m,150m,250m,350m,400m})	48.3	47.9	47.2	45.5	43.4
HFFR with variation of ICB (α=0.7, β=1, γ=0, δ=0.5, ICB={50m, 150m, 250m, 350m,400m})	43.5	42.3	40.4	36.9	34.9

The achieved results for different values of δ, in SFFR and HFFR cases, are shown in Fig. 9 and Fig. 10, respectively. It is noticed that with the reduction of δ, the overall PRB throughput on the cell border increases. In SFFR, PRB throughput gains at the cell border cause PRB throughput losses to occur in the cell centre. This was not the case for HFFR. In HFFR case, with the decrease of δ, gains were observed in the cell centre, as well as at the cell border.

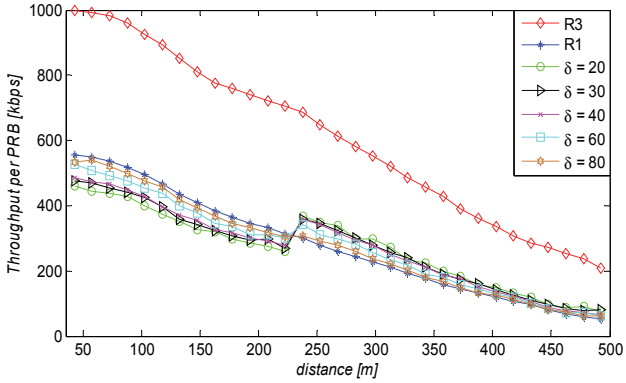

Fig. 9. The average throughput per PRB as a function of distance from BS, for SFFR with variation of δ.

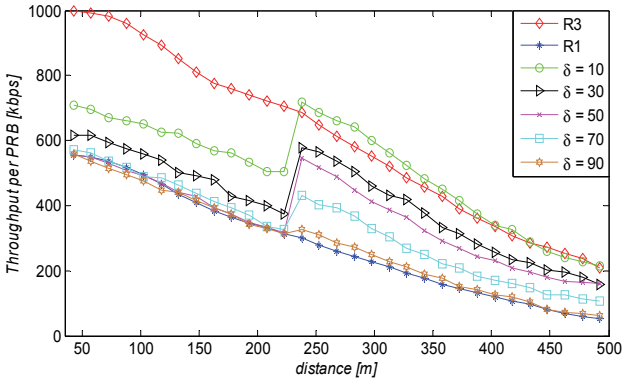

Fig. 10. The average throughput per PRB as a function of distance from BS, for HFFR with variation of δ.

The overall throughput decreases with the reduction of δ. In spite of larger gains in PRB throughput in HFFR case, overall throughput was much higher for SFFR. Those results were expected, because with the decrease of δ HFFR begins to resemble the R3 scheme. Besides that, HFFR has fewer available PRBs compared to SFFR and R1 schemes.

Achieved results for ICB, in SFR, SFFR and HFFR cases, are shown in Fig. 11, Fig. 12 and Fig. 13, respectively. In all schemes with the increase of ICB, PRB throughput for border users is increasing. In SFR and SFFR cases that increase has a direct impact on the reduction of PRB throughput for central users, just as it was in previous cases. In HFFR case there is a throughput increase for border users, but there are no throughput decreases for central users. In all cases, with an ICB decrease PRB throughput gravitates to the throughput for R1 and thus the overall cell throughput is increased. As expected, SFFR has the highest overall throughput because it most closely resembles the R1. This also implies that it has the smallest gains for border users, compared to other simulated schemes.

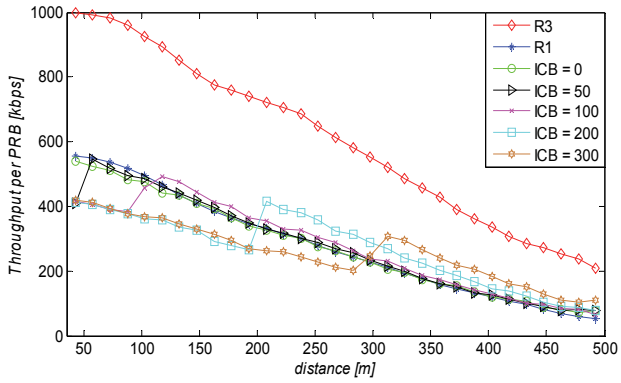

Fig. 11. The average throughput per PRB as a function of distance from BS, for SFR with variation of ICB.

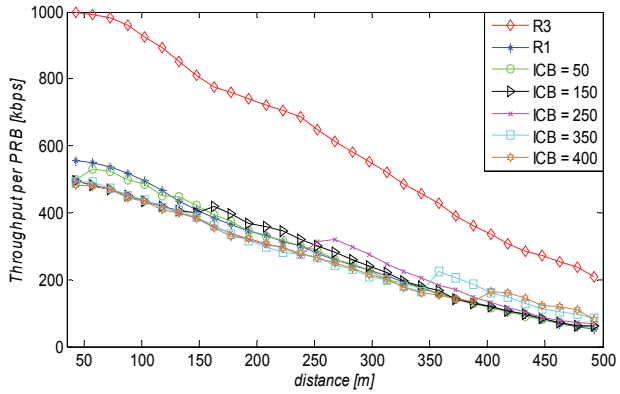

Fig. 12. The average throughput per PRB as a function of distance from BS, for SFFR with variation of ICB.

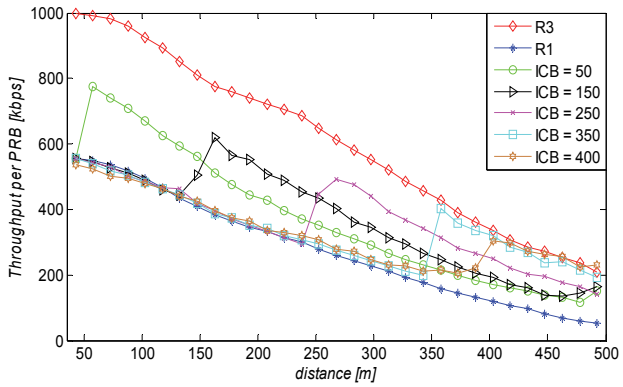

Fig. 13. The average throughput per PRB as a function of distance from BS, for HFFR with variation of ICB.

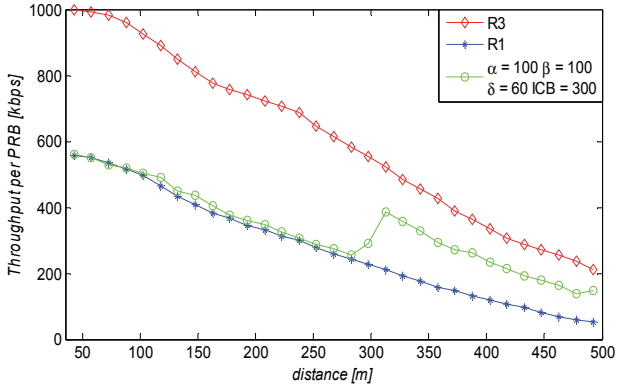

Fig. 14. The average throughput per PRB as a function of distance from BS, for proposed parameters.

Finally, it can be concluded that the HFFR scheme is the best way to allocate radio resources. This scheme achieves a significantly better overall throughput than the R3 scheme. Although HFFR achieves a lower overall throughput than SFR and SFFR schemes, it provides a much greater PRB throughput for border users, without inflicting losses for central users that occur in SFR and SFFR. By adjusting parameters δ and ICB, a much better PRB throughput on the cell border could be achieved compared to R1. To achieve a compromise between cell border throughput and the overall throughput, the parameter δ should be between 0.5 and 0.7, while the ICB should be between 50% and 70% of the cell radius. The parameter α can be set to 1. Doing so, enough power is left to the transmitter allowing good performances to be maintained, even in cases of the deterioration of propagation conditions. The total throughput for these parameters is 42.5 Mbps. PRB throughput, as a function of distance from BS, for this case is shown in Fig. 14.

V. Concluding Remarks

Based on the analysis conducted in this paper, it can be concluded that the best results are achieved with the HFFR allocation scheme. The HFFR scheme represents a good compromise between the overall cell throughput and the degree of interference suppression for users on the cell border. Taking that into account, it can be concluded that cell border users achieve a higher throughput in the HFFR scheme than they would using the R1 scheme.

Further research in this area could be the analysis of network radio resource allocation in realistic environments. A topic for further research could also be the analysis of performance of different allocation schemes depending on the number of users in a network.

References

[1] G. Boudreau, J. Panicker, N. Guo, R. Chang, N. Wang, and S. Vrzic, "Interference Coordination and Cancellation for 4G Network," *IEEE Communications Magazine* , vol. 47, no. 4, pp. 74-81, April 2009.

[2] N. Himayat, S. Talwar, A. Rao, and R. Soni, "Interference Management for 4G Cellular Standards," *IEEE Communications Magazine* , vol. 48, no. 8, pp. 86-92, August 2010.

[3] M. Rahman, H. Yanikomeroglu, and W. Wong, "Interference Avoidance with Dynamic Inter-Cell Coordination for Downlink LTE System," *Proc. of the Wireless Communications and Networking Conference (WCNC 2009),* Budapest, Hungary, April 2009.

[4] 3GPP. (2010, October 2). *Physical layer aspects for evolved Universal Terrestrial Radio Access (UTRA) (Release 7).* Accessed May 12, 2011 from 3GPP Specifications: http://www.3gpp.org/ftp/specs/2011-03/Rel-7/25_series/25814-710.zip

[5] I. Maravić, LTE Simulator source code, November 2011, accessed from: https://github.com/i-maravic/LTE-Simulator , March 21, 2012

[6] 3GPP. (2010, Septembar 17). *Multiplexing and channel coding (Release 9).* Accessed May 12, 2011 from 3GPP Specifications: http://www.3gpp.org/ftp/specs/2011-03/Rel-9/36_series/36212-930.zip

[7] 3GPP. (2010, Septembar 17). *Physical layer procedures (Release 9).* Acessed May 12, 2011 from 3GPP Specifications: http://www.3gpp.org/ftp/specs/2011-03/Rel-9/36_series/36213-930.zip

[8] C. Mehlführer, M. Wrulich, J.C. Ikuno, D. Bosanska, and M. Rupp, "Simulating the Long Term Evolution Physical Layer," *Proc. of the 17th European Signal Processing Conference (EUSIPCO 2009),* Glasgow, Scotland, 2009, accessed from http://publik.tuwien.ac.at/files/PubDat_175708.pdf , May 12, 2011.